IAC-12-C1.9.10

COUPLED ORBIT AND ATTITUDE DYNAMICS OF A RECONFIGURABLE SPACECRAFT WITH SOLAR RADIATION PRESSURE

Andreas Borggräfe
Advanced Space Concepts Laboratory, Department of Mechanical and Aerospace Engineering,
University of Strathclyde, Glasgow, Scotland G1 1XJ, United Kingdom,
E-Mail: andreas.borggraefe@strath.ac.uk

Matteo Ceriotti
School of Engineering, University of Glasgow, Glasgow, Scotland G12 8QQ, United Kingdom,
E-Mail: matteo.ceriotti@glasgow.ac.uk

Jeannette Heiligers
Advanced Space Concepts Laboratory, Department of Mechanical and Aerospace Engineering,
University of Strathclyde, Glasgow, Scotland G1 1XJ, United Kingdom,
E-Mail: jeannette.heiligers@strath.ac.uk

Colin R. McInnes
Advanced Space Concepts Laboratory, Department of Mechanical and Aerospace Engineering,
University of Strathclyde, Glasgow, Scotland G1 1XJ, United Kingdom,
E-Mail: colin.mcinnes@strath.ac.uk

This work investigates the orbital and attitude dynamics of future reconfigurable multi-panel solar sails able to change their shape during a mission. This can be enabled either by changing the relative position of the individual panels, or by using articulated mechanisms and deployable, retractable and/or inflatable structures. Such a model introduces the concept of modular spacecraft of variable morphology to large gossamer spacecraft. However, this joint concept is complex in nature and requires equations for coupled orbit/attitude dynamics. Therefore, as a starting point, the system is modelled as a rigid-body dumbbell consisting of two tip masses connected by a rigid, massless panel. The system is subjected to a central gravitational force field under consideration of solar radiation pressure forces. Therefore, we assign reflectivity coefficients to the tip masses and a high area-to-mass ratio. An analytical Hamiltonian approach is used to describe the planar motion of the system in Sun-centred Keplerian and non-Keplerian circular orbits. The stability and controllability of the system is enabled through changing the reflectivity coefficients, for example through the use of electro-chromic coating on its surface. The creation of artificial unstable equilibria of the system due to the presence of solar radiation pressure and heteroclinic connections between the equilibria are investigated. We further derive a constraint for the solar radiation pressure forces to maintain the system on a circular Sun-centred orbit. It is planned that the structure is eventually capable of reconfiguring between the equilibria by a minimum actuation effort.

I. INTRODUCTION

Solar sail technology offers a new capability to enable fast, efficient and low cost science missions throughout the Solar System. Solar sails exploit the flux of momentum transported by solar photons and thus do not require any propellant. The mission time is in principle only limited by the lifetime of the onboard subsystems and the integrity of the lightweight sail membrane. However, the solar radiation pressure (SRP) force vector is limited to be always directed away from the Sun and its magnitude follows an inverse square law with solar distance, making the sail less efficient at large distances from the Sun[1]. In order to increase the range of potential mission applications, it is envisaged to use the solar sail as a multi-functional platform that can deliver additional key mission functions such as power collection, sensing, communications and a more flexible SRP

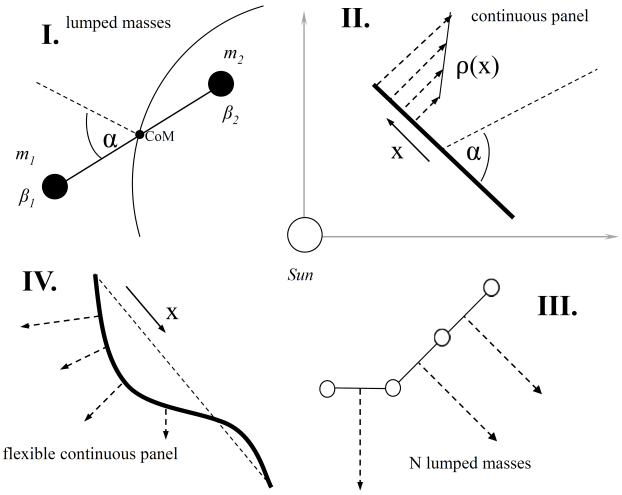

Figure 1: Modelling of reconfigurable gossamer spacecraft, segmented in phase I to IV

force vector control. For example, the sail could start at Earth in a flat configuration on a small body science mission towards a designated object like an asteroid or comet. In close proximity to the target body, the sail reconfigures to a parabolic shape, using its membrane as a remote sensing device, before continuing again in a flat thrust mode. Such a platform introduces the concept of modular spacecraft of variable morphology to large gossamer spacecraft[2,3]. In order to understand the dynamics of such reconfigurable spacecraft, the following roadmap defines a number of consecutive phases. As can be seen in Fig. 1, the identified phases gradually increase the complexity of the system, starting with a configuration of two lumped masses in phase I. After replacing the individual masses by a continuous panel in phase II, the number of masses will be increased in phase III to approximate a system of multiple possible shapes. In the last phase IV, the discrete n-body formation will again be replaced by a flexible continuous panel, offering a multifunctional platform for space missions.

The initial approach presented in this paper describes the planar motion of a rigid two-body dumbbell system in a Sun-centred orbit and under the effect of SRP forces. Hereby, we adapt the widely used model of a tethered satellite system (TSS)[4]. The SRP forces are introduced to the system as acting solely on the tip masses and only in radial direction away from the Sun, assigning a variable surface reflectivity to the masses. After describing the dynamical model in section II, we present the system's Hamiltonian and the equations of motion (EOM) for the coupled orbit/attitude motion in section III. By introducing a central bus mass, the EOM are further decoupled from the orbit (section IV). Under the assumption that the system's centre of mass (CoM) stays on a circular orbit, analytical formulations are derived in section IV.I for the decoupled case, showing that the relative equilibria depend on the reflectivity of the two masses. We demonstrate that through introduction of SRP forces to the problem, artificial equilibrium attitudes can be generated that vary from the ones well-known from the pure gravity gradient dumbbell[5]. In section IV.II, we are reintroducing the coupling of the orbit and attitude dynamics by deriving constraints for the reflectivity coefficients, showing that without the central bus mass, the dumbbell can also be maintained on a circular non-Keplerian orbit using SRP. The dynamical behaviour of the system is shown in section IV.III through equal energy curves of the Hamiltonian in phase space and a stability analysis. Within section IV.IV, motion between and controllability around the equilibria are demonstrated in the phase space of the problem through heteroclinic connections and by changing the surface reflectivity.

II. DYNAMICAL MODEL DESCRIPTION

The planar motion of the dumbbell system is described with respect to a Sun-centred inertial frame $\mathcal{I}:(X,Y)$ in the case of the coupled orbit/attitude problem and relative to a rotating orbit frame $\mathcal{O}:(r,t)$, originating in the CoM of the system for the decoupled attitude dynamics (Fig. 2). The axes of frame $\mathcal{O}$ are aligned with the local vertical and the local horizontal relative to the Sun.

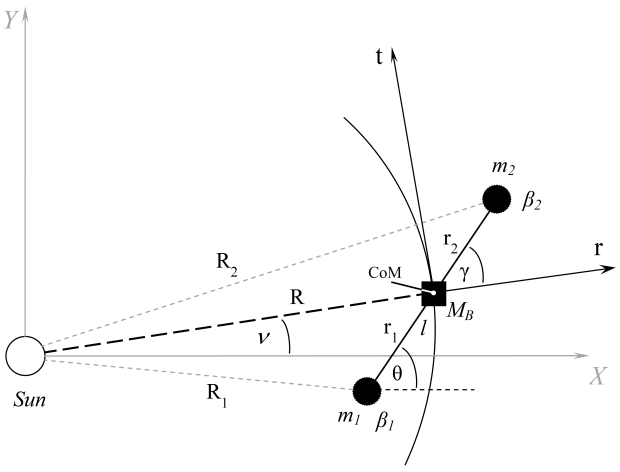

Figure 2: Geometry of dumbbell system in Sun-centred orbit with SRP forces

The system is modelled as a rigid body with a central bus mass M_B and two variable tip masses m_1 and m_2 at each end of a massless panel. The dimensionless dumbbell parameter $\lambda = l/R$ describes the ratio of panel length l to orbit radius R and the three bodies are approximated as point masses. M_B is located in the CoM of the system with $M_\mathrm{B} \gg m_i$. The dynamics within the

Sun's gravitational field are extended by introducing SRP forces to the two tip masses, assigning arbitrary lightness numbers $\beta_i = [0, 1]$. The lightness number of an object describes the ratio of its acceleration due to SRP and gravitational force. Bodies with a high surface reflectivity and a high area-to-mass ratio own a high value of β. Compared to the tip masses, the area-to-mass ratio of the central bus mass is assumed to be very small, so the lightness number of M_B can be neglected. The position vectors of the CoM and the two masses are described using time-dependent polar coordinates: the radial distance from the central body $R(t)$ and the true anomaly $\nu(t)$. Further, the angle $\theta(t)$ represents the dumbbell attitude relative to the inertial X-axis. In the following, the time variable t will be omitted to improve readability. For a rigid body, the position vector $\mathbf{R}$ of the CoM in the frame $\mathcal{I}$ is described as

$$\mathbf{R} = \frac{1}{M}\sum_{i=1}^{n} m_i \mathbf{R}_i \tag{1}$$

using the total mass $M = m_1 + m_2 + M_\mathrm{B}$. With respect to the inertial frame $\mathcal{I}$, the position vectors are

$$\mathbf{R} = R\begin{pmatrix}\cos\nu\\ \sin\nu\end{pmatrix} \tag{2a}$$

$$\mathbf{R}_1 = \mathbf{R} + \mathbf{r}_1, \qquad \mathbf{R}_2 = \mathbf{R} + \mathbf{r}_2 \tag{2b}$$

$$\mathbf{r}_1 = -\frac{m_2\, l}{m_1 + m_2}\begin{pmatrix}\cos\theta\\ \sin\theta\end{pmatrix} \tag{2c}$$

$$\mathbf{r}_2 = \frac{m_1\, l}{m_1 + m_2}\begin{pmatrix}\cos\theta\\ \sin\theta\end{pmatrix} \tag{2d}$$

The norms of the position vectors are

$$R_1 = \sqrt{R^2 - \frac{2 l m_2 R\cos(\nu-\theta)}{m_1+m_2} + \left(\frac{l m_2}{m_1+m_2}\right)^2} \tag{3a}$$

$$R_2 = \sqrt{R^2 + \frac{2 l m_1 R\cos(\nu-\theta)}{m_1+m_2} + \left(\frac{l m_1}{m_1+m_2}\right)^2} \tag{3b}$$

III. COUPLED EQUATIONS OF MOTION

The coupled orbit/attitude EOM of the two-mass dumbbell are derived through formulation of the system's Hamiltonian in the inertial frame[6]. Using the Euler-Lagrange equations, the coupled EOM are formulated using the second derivatives $\ddot{R}(t)$, $\ddot{\nu}(t)$ and $\ddot{\theta}(t)$.

Potential and Kinetic Energy

Within the potential energy function, the SRP forces are added to the gravitational forces. We assume that the SRP force on the tip masses solely acts in radial direction. As a result of this assumption, the SRP forces may be included into the potential energy function, since they are supposed to originate from a conservative force field. Introducing a so called effective gravitational parameter $\tilde{\mu}_i = \mu(1-\beta_i)$ for each mass within the potential energy function, this parameter represents the reduced effect of the gravitational force due to a radially outward SRP force. The effective potential energy V of the system can now be written as

$$\begin{aligned} V = &-\frac{\mu M_\mathrm{B}}{R} - \sum_{i=1}^{2}\frac{\tilde{\mu}_i m_i}{R_i} = \\ &-\frac{\mu M_\mathrm{B}}{R} - \frac{\mu m_1(1-\beta_1)}{R_1} - \frac{\mu m_2(1-\beta_2)}{R_2} \end{aligned} \tag{4}$$

Note that, recalling the above expressions for the norms R_i from Eq. 3, the effective potential energy of the SRP dumbbell depends on the radial position R of the CoM, the angles ν and θ, the masses m_i and the lightness numbers β_i.

The kinetic energy is split up into a translational part T_transl attached to the CoM and a rotational part T_rot, representing the contribution of the two rotating masses to the total kinetic energy

$$T_\text{transl} = \frac{1}{2}M\dot{\mathbf{R}}\dot{\mathbf{R}} = \frac{1}{2}(m_1+m_2+M_\mathrm{B})(\dot{R}^2 + R^2\dot{\nu}^2) \tag{5a}$$

$$\begin{aligned} T_\text{rot} &= \frac{1}{2}\sum_{i=1}^{2} m_i\dot{\mathbf{r}}_i\dot{\mathbf{r}}_i = \frac{1}{2}m_1\dot{\mathbf{r}}_1\dot{\mathbf{r}}_1 + \frac{1}{2}m_2\dot{\mathbf{r}}_2\dot{\mathbf{r}}_2 \\ &= \frac{1}{2}\frac{m_1 m_2 l^2}{m_1+m_2}\dot{\theta}^2 \end{aligned} \tag{5b}$$

Coupled Hamiltonian

Using the Lagrangian $L = T - V$ and introducing three generalized coordinates $q_i = (R, \nu, \theta)$, the Hamiltonian of the dynamical system can be written as

$$H = \sum_{i=1}^{3}\frac{\partial L}{\partial \dot{q}_i}\dot{q}_i - L = \dot{R}\frac{\partial L}{\partial \dot{R}} + \dot{\nu}\frac{\partial L}{\partial \dot{\nu}} + \dot{\theta}\frac{\partial L}{\partial \dot{\theta}} - L \tag{6}$$

In this approach, no non-conservative external forces are acting on the system and time does not appear explicitly in the expressions for the potential and kinetic energy, so the Hamiltonian is a constant of motion[7]. Calculating the

generalized momenta p_i

$$p_1 = \frac{\partial L}{\partial \dot{R}} = (m_1{+}m_2{+}M_\mathrm{B})\dot{R} \tag{7a}$$

$$p_2 = \frac{\partial L}{\partial \dot{\nu}} = (m_1{+}m_2{+}M_\mathrm{B})R^2\dot{\nu} \tag{7b}$$

$$p_3 = \frac{\partial L}{\partial \dot{\theta}} = \frac{m_1 m_2 l^2}{m_1{+}m_2}\dot{\theta} \tag{7c}$$

the non-dimensional coupled Hamiltonian $\hat{H}$ of the system is found after dividing H by $\frac{1}{2}(m_1{+}m_2)\dot{\nu}^2 l^2$

$$\hat{H} = \frac{2}{(m_1{+}m_2)\dot{\nu}^2 l^2}\left[\frac{1}{2}(m_1{+}m_2)(\dot{R}^2 + R^2\dot{\nu}^2) + \frac{1}{2}\frac{m_1 m_2 l^2}{m_1{+}m_2}\dot{\theta}^2 - \frac{\mu m_1(1{-}\beta_1)}{R_1} - \frac{\mu m_2(1{-}\beta_2)}{R_2}\right] \tag{8}$$

Note that the coupled Hamiltonian $\hat{H}$ is a function of the free parameters β_i, besides the dumbbell parameters m_i and l.

Euler-Lagrange Equations

According to Hamilton's principle and using the generalized coordinates $q_k(t)$, $k = 1, ..., n$, the trajectory of $q(t) = (q_1(t), ..., q_n(t))$ through the configuration space satisfies the Euler-Lagrange equations[7]

$$\frac{\mathrm{d}}{\mathrm{d}t}\left(\frac{\partial L}{\partial \dot{q}_i}\right) - \frac{\partial L}{\partial q_i} = 0 \tag{9}$$

Using the above equation, the coupled EOM of the two-mass dumbbell including SRP can be formulated as

$$\ddot{R} + \frac{\mu M_\mathrm{B}}{MR^2} + \frac{\mu m_1(1{-}\beta_1)\left(R - \frac{l m_2\cos(\theta{-}\nu)}{m_1{+}m_2}\right)}{MR_1^3} + \frac{\mu m_2(1{-}\beta_2)\left(R + \frac{l m_1\cos(\theta{-}\nu)}{m_1{+}m_2}\right)}{MR_2^3} - R\dot{\nu}^2 = 0 \tag{10a}$$

$$\ddot{\nu} + \frac{\mu m_1 m_2 l\sin(\theta{-}\nu)}{M(m_1{+}m_2)\,R}\left(\frac{(1{-}\beta_2)}{R_2^3} - \frac{(1{-}\beta_1)}{R_1^3}\right) + \frac{2\dot{R}\dot{\nu}}{R} = 0 \tag{10b}$$

$$\ddot{\theta} + \frac{\mu\,R\sin(\theta{-}\nu)}{l}\left(\frac{(1{-}\beta_1)}{R_1^3} - \frac{(1{-}\beta_2)}{R_2^3}\right) = 0 \tag{10c}$$

IV. DECOUPLED EQUATIONS OF MOTION

Assuming a central bus mass $M_\mathrm{B} \gg m_i$, it can be shown that the attitude motion of the system decouples from the orbit dynamics, thus Eqs. 10a and 10b reduce to the common 2-B-P of a single mass in a central gravitational field and no longer depend on the dumbbell attitude θ. Introducing the above condition for M_B into Eq. 10 results in the decoupled EOM of the dumbbell including SRP

$$\ddot{R} + \frac{\mu}{R^2} - R\dot{\nu}^2 = 0 \tag{11a}$$

$$\ddot{\nu} + \frac{2\dot{R}\dot{\nu}}{R} = 0 \tag{11b}$$

$$\ddot{\theta} + \frac{\mu\,R\sin(\theta{-}\nu)}{l}\left(\frac{(1{-}\beta_1)}{R_1^3} - \frac{(1{-}\beta_2)}{R_2^3}\right) = 0 \tag{11c}$$

When the CoM of the system initially follows a circular orbit with $\dot{\nu} = \sqrt{\mu/R^3}$ and $\dot{R} = 0$, Eqs. 11a and 11b further reduce to $\ddot{R} = 0$ and $\ddot{\nu} = 0$, respectively. The true anomaly ν is a cyclic variable and arbitrary (including zero) along a circular orbit, thus Eq. 11c can now be written as

$$\ddot{\theta} + \frac{\mu\,R\sin\theta}{l}\left(\frac{(1{-}\beta_1)}{R_1^3} - \frac{(1{-}\beta_2)}{R_2^3}\right) = 0 \tag{12}$$

The same decoupled attitude EOM (Eq. 12) can be obtained through derivation of the system's Hamiltonian in the rotating orbit frame $\mathcal{O}:(r,t)$, without considering the central mass M_B, as shown in Figure 3. This second approach for the decoupled problem is given to show that the resulting attitude EOM is consistent with the one obtained from the introduction of M_B before.

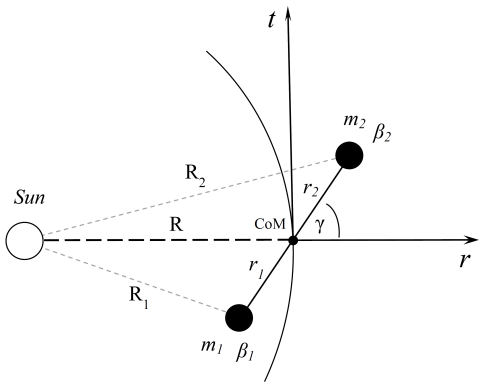

Figure 3: Geometry of dumbbell system with SRP for the decoupled attitude problem with respect to the rotating orbit frame $\mathcal{O}:(r,t)$, centred in the CoM

The dumbbell attitude is now described using the angle γ with respect to the local vertical. The CoM is again assumed to move along a circular orbit with angular velocity ω. Without using M_B as before, this only holds true for very small ratios $\lambda \ll 1$. However, we will show later that a constraint can be introduced to the lightness numbers β_i to satisfy this assumption exactly (see section IV.II). In the rotating orbit frame $\mathcal{O}$, the relative position of the CoM is always

$$\mathbf{r}_{\text{CoM}} = \frac{1}{m_1+m_2}\sum_{i=1}^{n} m_i \mathbf{r}_i = 0 \tag{13}$$

For the decoupled problem, the position vectors are transformed into the rotating frame, using $\mathbf{R} = (R,0)^T$ for the CoM and the position vectors $\mathbf{R}_i$ now being a function of the angle γ

$$\mathbf{R}_1 = \mathbf{R} + \mathbf{r}_1 = \begin{pmatrix} R \\ 0 \end{pmatrix} - \frac{m_2}{m_1+m_2} l \begin{pmatrix} \cos\gamma \\ \sin\gamma \end{pmatrix} \tag{14a}$$

$$\mathbf{R}_2 = \mathbf{R} + \mathbf{r}_2 = \begin{pmatrix} R \\ 0 \end{pmatrix} + \frac{m_1}{m_1+m_2} l \begin{pmatrix} \cos\gamma \\ \sin\gamma \end{pmatrix} \tag{14b}$$

Potential and Kinetic Energy

For the decoupled case, only the rotational part of the kinetic energy

$$T_{\text{rot}} = \frac{1}{2}\frac{m_1 m_2 l^2}{m_1+m_2}(\dot{\gamma}^2 + 2\dot{\gamma}\omega + \omega^2) \tag{15}$$

is considered. The potential energy is used again as described before in the coupled case (Eq. 4, with $M_B = 0$). However, since now only the attitude motion of the dumbbell is considered, the orbital potential energies of the CoM due to gravitational and SRP forces

$$V_{\text{orb}} = -\frac{\mu(m_1+m_2)}{R},\ V_{\text{orb,SRP}} = \frac{\mu(m_1\beta_1+m_2\beta_2)}{R} \tag{16}$$

are substracted from V within the decoupled Lagrangian

$$L_{\text{dec}} = T_{\text{rot}} - V_{\text{rot}} = T_{\text{rot}} - (V - V_{\text{orb}} - V_{\text{orb,SRP}}) \tag{17}$$

Decoupled Hamiltonian

The Hamiltonian H_{dec} is now reformulated using only $q_1 = \gamma$ as the generalized coordinate. With the corresponding generalized momentum

$$p_1 = \frac{\partial L}{\partial \dot{\gamma}} = \frac{m_1 m_2 l^2(\dot{\gamma}+\omega)}{m_1+m_2} \tag{18}$$

the non-dimensional Hamiltonian $\hat{H}_{\text{dec}}$ is found as

$$\begin{aligned}\hat{H}_{\text{dec}} = \frac{2}{(m_1+m_2)\omega^2 l^2}\Bigg[&\frac{1}{2}\frac{m_1 m_2 l^2}{m_1+m_2}(\dot{\gamma}^2-\omega^2) \\ &+ \frac{\mu(m_1+m_2)}{R} - \frac{\mu(m_1\beta_1+m_2\beta_2)}{R} \\ &- \frac{\mu m_1(1-\beta_1)}{R_1} - \frac{\mu m_2(1-\beta_2)}{R_2}\Bigg]\end{aligned} \tag{19}$$

Using again Eq. (9), the decoupled EOM of the dumbbell with SRP can be written in terms of the attitude angle γ in the rotating frame $\mathcal{O}$

$$\ddot{\gamma} + \frac{\mu R\sin\gamma}{l}\left(\frac{1-\beta_1}{R_1^3} - \frac{1-\beta_2}{R_2^3}\right) = 0 \tag{20}$$

as equivalent to Eq. 12, and in expanded notation

$$\begin{aligned}\ddot{\gamma} + \frac{\mu R\sin\gamma}{l}\Bigg[&\\ &\frac{1-\beta_1}{\left(R^2 - 2R\frac{m_2 l}{m_1+m_2}\cos\gamma + \left(\frac{m_2 l}{m_1+m_2}\right)^2\right)^{\frac{3}{2}}} \\ &- \frac{1-\beta_2}{\left(R^2 + 2R\frac{m_1 l}{m_1+m_2}\cos\gamma + \left(\frac{m_1 l}{m_1+m_2}\right)^2\right)^{\frac{3}{2}}}\Bigg] = 0\end{aligned} \tag{21}$$

IV.I EQUILIBRIUM ANGLES AND STABILITY

In this section, we show that the relative equilibria of the rigid-body dumbbell system in terms of the angle γ_{eq} are changing with β_1 and β_2. For both lightness numbers being zero and a mass ratio of $\kappa = 1$, the equilibrium angles are $\pm 180, \pm 90$ and 0 degrees and correspond to the pure gravity gradient dumbbell without SRP. Before introducing a suitable control strategy to move from one equilibrium state to another, the dependence of γ_{eq} on the two β-values is described. The dumbbell is in an equilibrium state whenever the total torque on the system is zero and thus, the total angular acceleration $\ddot{\gamma}$ is zero. Solving the decoupled attitude EOM (Eq. 20) for $\ddot{\gamma} = 0$ gives the equilibrium angle as a function of β_1, β_2 and the masses m_1, m_2

$$\begin{aligned}\gamma_{\text{eq}} = \arccos\Bigg[&-\frac{(1-\beta_1)^{\frac{2}{3}}\left(1+\left(\frac{m_1\lambda}{m_1+m_2}\right)^2\right)}{\left[(1-\beta_1)^{\frac{2}{3}}\left(\frac{2m_1\lambda}{m_1+m_2}\right)+(1-\beta_2)^{\frac{2}{3}}\left(\frac{2m_2\lambda}{m_1+m_2}\right)\right]} \\ &+ \frac{(1-\beta_2)^{\frac{2}{3}}\left(1+\left(\frac{m_2\lambda}{m_1+m_2}\right)^2\right)}{\left[(1-\beta_1)^{\frac{2}{3}}\left(\frac{2m_1\lambda}{m_1+m_2}\right)+(1-\beta_2)^{\frac{2}{3}}\left(\frac{2m_2\lambda}{m_1+m_2}\right)\right]}\Bigg]\end{aligned} \tag{22}$$

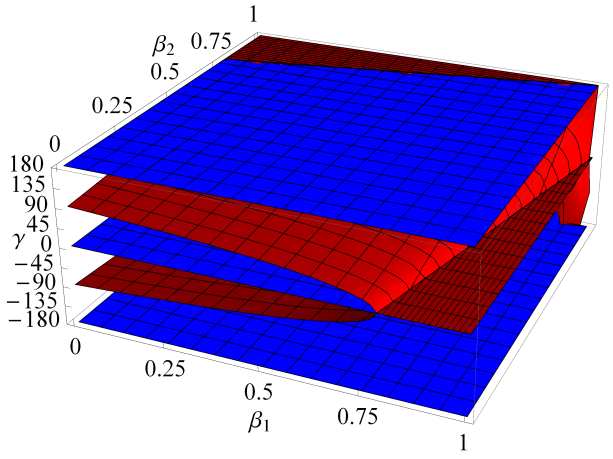

Figure 4: Stable (blue) and unstable (red) equilibria γ_{eq} as a function of β_1 and β_2 for the reference dumbbell with $\lambda = 0.5$

and further as a function of the dimensionless parameter $\lambda = l/R$, the dumbbell length/orbit ratio.

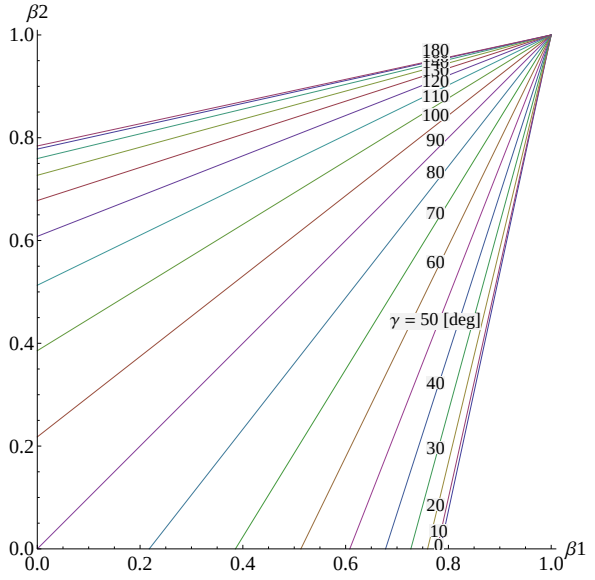

Figure 5: Possible $(\beta_1, \beta_2)_{\gamma_{eq}}$ sets to create unstable equilibria γ_{eq} for the reference dumbbell with $\lambda = 0.5$

In order to evaluate the stable/unstable character of the equilibria γ_{eq}, a stability analysis of the decoupled attitude EOM is applied. At first, the 2nd order differential equation given in Eq. (20) is linearized around γ_{eq} through a Taylor series expansion up to 1st order terms. Rewriting leads to a linear differential equation system (DES) of 1st order. When analysing the eigenvalues of the Jacobian of the DES, two different types of equilibria are obtained: unstable saddle and stable centre. In the following, the new equilibria of the dumbbell system that can be created when including SRP are investigated. Fig. 4 shows the stable (blue) and unstable (red) regions of equilibria γ_{eq} as a function of β_1 and β_2 for a chosen reference dumbbell with a very high $\lambda = 0.5$ and equal masses $m_1 = m_2$. The three planes are indicating the stable equilibria -180, 0 and 180 degrees. It can be seen that for large values of one of the lightness numbers, the stable equilibria are transformed into unstable ones, similar to the pure gravity gradient dumbbell configuration with a very large/small mass ratio $\kappa = m_1/m_2$. The two red curved planes indicate new unstable equilibria. Choosing β_1 and β_2 in the range of $[0, 1]$ reduces the net effective gravitational force on each mass from its usual value of μ/R_i^2 to zero. Both effects of the gravity gradient and the SRP force are proportional to $1/R^2$ or l^2, respectively. Further, only the difference between the forces acting on m_1 or m_2 are influencing the dynamical and static behaviour of the system, by causing a resulting net torque about the CoM. In order to magnify the effect of the combined gravity and SRP gradient, a dumbbell with a high λ is chosen for illustration.

When solving Eq. (22) for β_2, the possible combinations $(\beta_1, \beta_2)_{\gamma_{eq}}$ for a given equilibrium angle, further referred to as 'β-sets', can be obtained as

$$\beta_2(\beta_1, \gamma_{eq}) = 1 - \left[\frac{\left[1 + \left(\frac{m_1\lambda}{m_1+m_2}\right)^2\right](1-\beta_1)^{\frac{2}{3}} - \frac{2m_1\lambda}{m_1+m_2}\cos\gamma\,(1-\beta_1)^{\frac{2}{3}}}{1 - \frac{2m_2\lambda}{m_1+m_2}\cos\gamma + \left(\frac{m_2\lambda}{m_1+m_2}\right)^2} \right]^{\frac{3}{2}} \tag{23}$$

For the chosen reference dumbbell and for equilibrium angles in the interval $[0, 180]$ degrees, the possible $(\beta_1, \beta_2)_{\gamma_{eq}}$ sets are shown in Fig. 5, parametrized in steps of $\Delta\gamma = 10$ degrees. Each point on one of the curves can be chosen to create a respective unstable equilibrium attitude γ_{eq}.

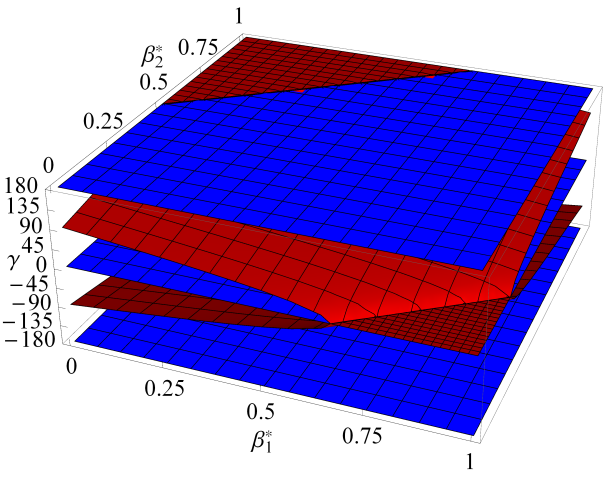

Figure 6: Stable (blue) and unstable (red) equilibria γ_{eq} as a function of scaled β_1^* and β_2^* for a dumbbell with ratio $\lambda = 1.7\times10^{-7}$

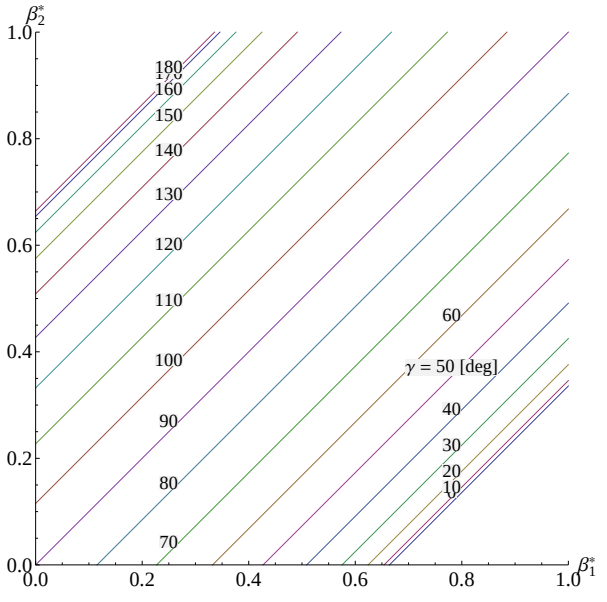

Figure 7: Possible $(\beta_1, \beta_2)_{\gamma_{\text{eq}}}$ sets to create unstable equilibria γ_{eq} for a dumbbell with ratio $\lambda = 1.7 \times 10^{-7}$

As a more realistic case, a dumbbell configuration with equal masses $m_1 = m_2$ and a dumbbell ratio $\lambda = 1.7 \times 10^{-7}$ is used in Figs. 6 and 7. For example, this ratio corresponds to a panel length $l = 10$ km on a circular Mercury orbit of radius $R = 57,909,100$ km. Both plots are scaled with a threshold for $\beta_i = 5.2 \times 10^{-7} \beta_i^*$ with $\beta_i^* = [0, 1]$ to improve readability, but the dumbbell can also be controlled over the full range of $\beta_i = [0, 1]$.

IV.II CONSTRAINTS ON SRP TO MAINTAIN CIRCULAR ORBIT

The decoupled EOM are only valid under the assumption that the CoM of the system stays on a circular orbit. This can be approximated when introducing the condition $\lambda \ll 1$ or a central bus mass. However, any lightness number assigned to the masses will cause the system to depart from the circular orbit, since through the additional SRP forces acting exactly in the opposite direction towards the gravitational forces, the force field is no longer a central Newtonian. The effect of the SRP is to decrease the effective solar gravity experienced by the dumbbell, as shown earlier by the introduction of $\tilde{\mu} = \mu(1-\beta_i)$. This means that any mass with a $\beta_i > 0$ on an originally circular heliocentric Keplerian orbit of radius R and orbit rate ω_0 will experience a reduced net force compared to the one from pure solar gravity at the same distance. As a result, the body will depart from the circular reference orbit in radial outward direction, since it is moving faster than the local effective angular velocity $\tilde{\omega} = \sqrt{\tilde{\mu}/R^3}$ of the circular non-Keplerian orbit. However, when the mass is orbiting with this reduced $\tilde{\omega}$, it can maintain a circular non-Keplerian orbit of same radius R. We now derive a constraint for β_1 and β_2 acting on the two masses that allows the CoM of the system to stay on a given circular reference orbit and hereby reintroduce the coupling of the orbit and attitude dynamics. To this aim, the sum of the forces for the two-mass dumbbell body formulated in the rotating frame $\mathcal{O}$ shall be equal to the sum of forces acting on a virtual reference single-mass body of total mass $M_{\text{CoM}} = m_1 + m_2$. The CoM of both bodies is located on the same circular reference orbit of radius R. Formulating with respect to the orbit frame $\mathcal{O}$ gives

$$-\frac{\mu m_1(1-\beta_1)}{R_1^3}\mathbf{R}_{1,\text{rot}} - \frac{\mu m_2(1-\beta_2)}{R_2^3}\mathbf{R}_{2,\text{rot}} = -\frac{\tilde{\mu}_{\text{CoM}}\, M_{\text{CoM}}}{R^3}\mathbf{R}_{\text{rot}} = \text{const.} \tag{24}$$

The orbit of the reference mass is assumed to be non-Keplerian by using an effective gravitational parameter $\tilde{\mu}_{\text{CoM}} = \mu(1-\beta_{\text{CoM}})$ with β_{CoM} being a lightness number assigned to the reference mass. It is a free parameter that defines the orbital angular velocity $\tilde{\omega}_{\text{CoM}} = \sqrt{\tilde{\mu}_{\text{CoM}}/R^3}$ necessary to stay on the non-Keplerian circular reference orbit. For a given dumbbell with parameters m_1, m_2 and λ, Eq. 24 is a function of the two lightness numbers. Solving in the radial and transversal direction results in two constraint equations for β_1 and β_2

$$\beta_1 = \frac{1 - \frac{\tilde{\mu}_{\text{CoM}}}{\mu}\frac{m_1+m_2}{m_2 R^2}\frac{R_1^3}{R_{2,\text{r}}} + \frac{m_1}{m_2}\frac{R_{1,\text{r}}}{R_{2,\text{r}}}}{1 + \frac{m_1}{m_2}\frac{R_{1,\text{r}}}{R_{2,\text{r}}}} = \text{f}_1(\gamma) \tag{25a}$$

$$\beta_2 = \frac{1 - \frac{\tilde{\mu}_{\text{CoM}}}{\mu}\frac{m_1+m_2}{m_2 R^2}\frac{R_2^3}{R_{2,\text{r}}} + \frac{m_1}{m_2}\frac{R_{1,\text{r}}}{R_{2,\text{r}}}}{1 + \frac{m_1}{m_2}\frac{R_{1,\text{r}}}{R_{2,\text{r}}}} = \text{f}_2(\gamma) \tag{25b}$$

with $R_{\text{i,r}}$ the radial components of the position vectors of the two masses (Eq. 14). Note that above equations are coupled through the angle γ, thus for any relative attitude of the dumbbell and a given circular reference orbit, the constrained β-set for the two masses is now completely defined. Figs. 8 and 9 show the constrained $(\beta_1, \beta_2)_{\gamma_{\text{eq}}}$ sets over the range of equilibrium angles $[-180, 180]$ degrees. A family of circular non-Keplerian orbits with decreasing orbit rates $\tilde{\omega} < \omega_0$ is used, starting with $\omega_0 = \sqrt{\mu/R^3}$ for the reference circular Keplerian orbit with radius R. Again, the reference dumbbell with $\lambda = 0.5$ and equal masses $m_1 = m_2$ is used. It can be seen in the figures that in case of the reference Keplerian orbit (blue line) it is not possible to create any equi-

librium states without departing from the circular orbit, since the β_i have opposite signs for all γ_{eq} within the range of $[-180, 180]$ degrees and a negative β can not be created from a radial outward SRP force. When decreasing the orbital rate to $\tilde{\omega} = 0.9, 0.8$ and $0.7\,\omega_0$ (as seen in Figs. 8 and 9), the region of possible equilibria can be increased gradually. For $\tilde{\omega} = 0.7\,\omega_0$, all equilibrium attitudes are possible.

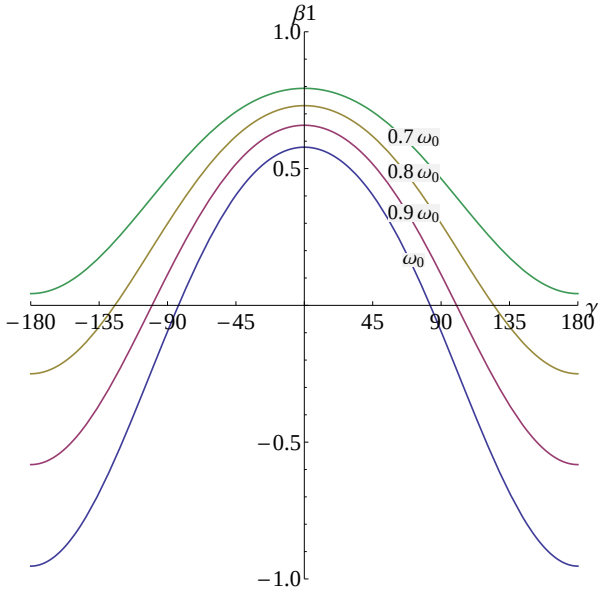

Figure 8: Constrained β_1 for the reference dumbbell including SRP to maintain a circular orbit for a given equilibrium angle γ_{eq}

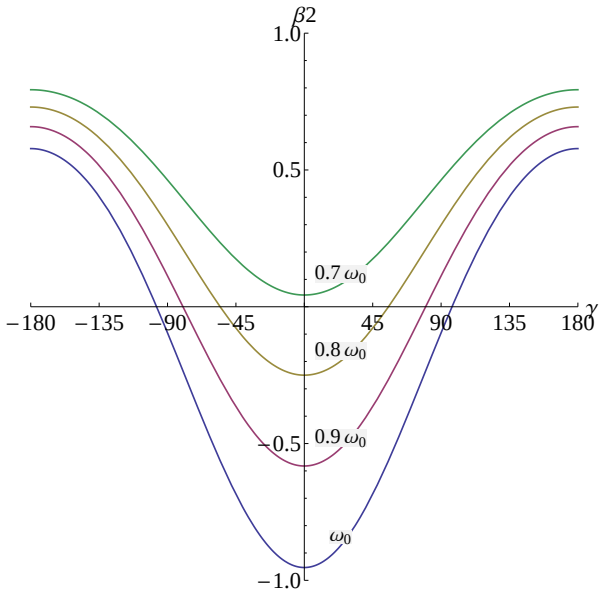

Figure 9: Constrained β_2 for the reference dumbbell including SRP to maintain a circular orbit for a given equilibrium angle γ_{eq}

This non-Keplerian orbit is equivalent to the one created when assigning a lightness number of $\beta_{CoM} = 0.51$ to a reference single body with total mass M_{CoM}. The introduction of the new β-constraints in addition to the previously defined sets of possible β-values for the reference dumbbell (Fig. 5) is now visible in Fig. 10. While the possible $(\beta_1, \beta_2)_{\gamma_{eq}}$ sets for an equilibrium was a line for $\beta_i = [0, 1]$, the constraint now restricts the sets to one point, depending on the chosen orbit rate $\tilde{\omega}$ of the non-Keplerian circular orbit.

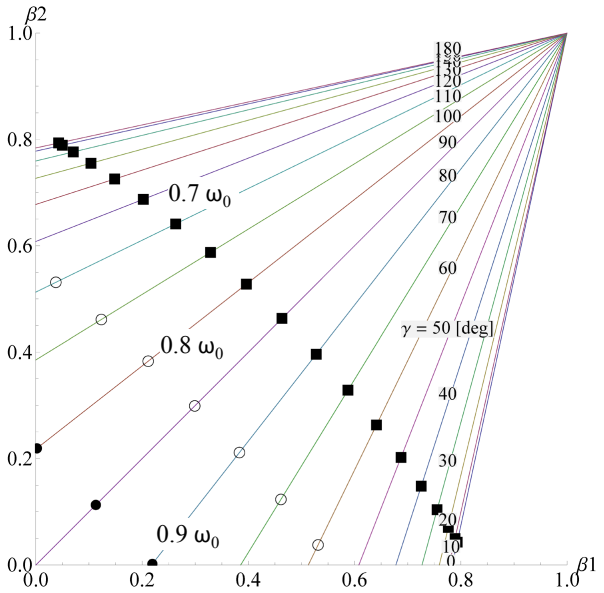

Figure 10: Possible $(\beta_1, \beta_2)_{\gamma_{eq}}$ sets for the reference dumbbell including SRP to create a given equilibrium angle γ_{eq} and superimposed β-constraint for various circular non-Keplerian orbits

IV.III PHASE SPACE OF THE PROBLEM

In the following, the dynamics of the decoupled problem are analysed using the above lightness-number constraint that allows the CoM of the dumbbell to stay on a circular non-Keplerian orbit with an orbital rate of $\tilde{\omega} < \omega_0$. Since the decoupled Hamiltonian is a constant of motion, for each value of $\hat{H}_{dec}$, the motion of the system is represented by a two-dimensional phase space $(\gamma, \dot{\gamma})$ with free parameters β_1 and β_2. Fig. 11 shows the equal energy curves in the phase space for the reference dumbbell configuration with $\lambda = 0.5$ and equal masses $m_1 = m_2$. Arrows indicate the direction of motion along a curve. Whenever the curves are closed, they correspond to librations around the equilibrium point. The open curves in the phase space correspond to rotations. Two superimposed phase spaces for different β-sets and the respective location of the stable and unstable equilibria are visible. The first set $(\beta_1, \beta_2)_1 = (0, 0)$ (black

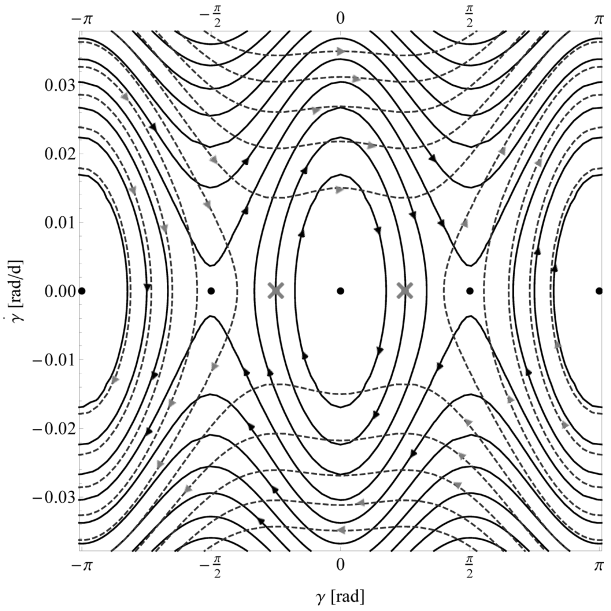

Figure 11: Superimposed phase spaces $[\gamma, \dot{\gamma}]$ of pure dumbbell without SRP forces $(\beta_1, \beta_2)_1 = (0, 0)$ (black solid curves) and with lightness numbers $(\beta_1, \beta_2)_2 = (0.71, 0.18)$ (dashed grey curves) on a reference Earth orbit. The stable and unstable equilibria are shown together with equal energy curves and arrows indicate the direction of motion along a curve

solid curves) corresponds to the pure gravity-gradient dumbbell without SRP, showing the unstable equilibria at +/-90 degrees, together with the stable ones at -180, 0 and 180 degrees (black points). The second set (grey dashed curves) is chosen according to the derived β-constraint for restricting the dumbbell on a circular non-Keplerian orbit (section IV.II). Here, as an example, the lightness numbers of the two masses are supposed to shift the unstable equilibria to ± 45 degree (grey crosses). For a chosen reference Earth orbit with radius $R_0 = 149,598,261$ km and orbital angular velocity $\omega_0 = 0.0172$ rad/day $(0.986$ deg/day), the non-Keplerian orbit in terms of orbital rate $\tilde{\omega}$ and the corresponding set $(\beta_1, \beta_2)_2$ that creates the ± 45 degree equilibria can be chosen from Figs. 8 and 9. An orbit with angular velocity $\tilde{\omega} = 0.7\,\omega_0 = 0.0120$ rad/day $(0.689$ deg/day) allows for positive β-sets in the full range of attitudes between $[-180, 180]$ degree. Accordingly, the resulting β-set is chosen to be $(\beta_1, \beta_2)_2 = (0.71, 0.18)$. Within the next section, we show possible controlled motion in phase space through changes in β_1 and β_2. Hereby, the dumbbell attitude can be changed and maintained just by using solar radiation pressure.

IV.IV MOTION IN PHASE SPACE

The phase space $(\gamma, \dot{\gamma})$ of the dumbbell system, including the positions of the respective equilibria, is characteristic for a particular β-set. Switching to another set, the phase space and the respective equilibria change accordingly, as seen in the previous section IV.III. We now exploit these attributes of the system to find heteroclinic connections between equilibria in the phase space. By providing a qualitative switching law between different β-sets, we aim towards arbitrarily changing the attitude of the dumbbell and further controlling it in the vicinity of a desired (unstable) attitude.

When inspecting again the superimposed phase space curves for two different β-sets as shown in Fig. 11, possible sequences in phase space in order to change the dumbbell attitude can be obtained. Whenever the dumbbell is in a state at (or close to) an unstable equilibrium (saddle), there a two directions in phase space for the system to move away from the saddle. The other two directions always lead towards the unstable point, as can be seen in Fig. 12.

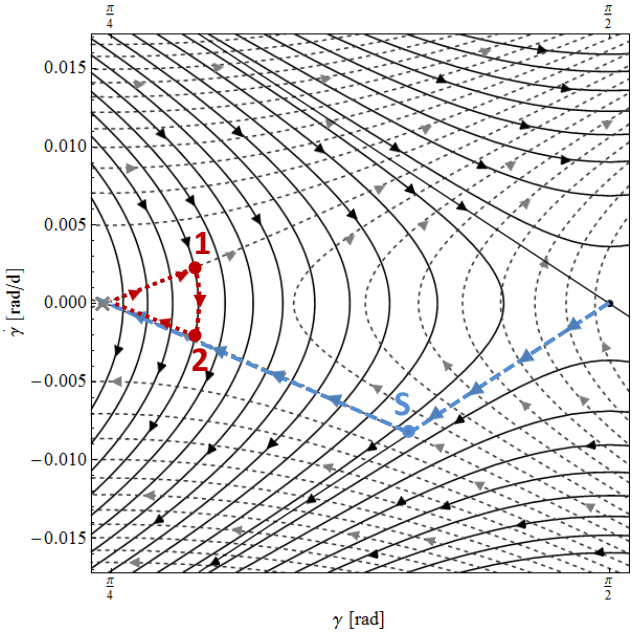

Figure 12: Detail view of superimposed phase spaces $[\gamma, \dot{\gamma}]$ of pure dumbbell without SRP forces $(\beta_1, \beta_2)_1 = (0, 0)$ (black solid curves) and with lightness numbers $(\beta_1, \beta_2)_2 = (0.71, 0.18)$ (dashed grey curves). Two possible sequences are highlighted: attitude change between unstable equilibria (blue dashed curve) and control sequence around an unstable equilibrium (red dotted curve)

For example, the system can move along the blue dashed curve away from the +90 degree saddle, as indicated through the blue arrows in the figure. Likewise, there are also two directions leading towards the +45 degree saddle of the second phase space (dashed grey lines). When switching between β-set 1 and 2 at the point in phase space indicated with a blue 'S', the dumbbell will consequently change its attitude from +90 to +45 degrees,

when following the blue path. In order to further control the dumbbell in the vicinity of an unstable saddle point, a motion sequence such as the one indicated with the red dotted curve can be used. When the system initially moves away from the saddle on one of the outgoing curves (within phase space 2), then switching to β-set 1 (black solid curves) at the point marked with a red '1' will let it further move along the closed loop around the stable centre of phase space 1. When it reaches point '2', which is the crossing with the ingoing curve towards the saddle, switching again to β-set 2 will complete a closed loop around the desired unstable equilibrium of +45 degree.

V. CONCLUSIONS

In this paper an analytical Hamiltonian approach was used to describe the planar motion of a rigid-body dumbbell system including solar radiation pressure (SRP) forces on the two masses on circular Sun-centred Keplerian and non-Keplerian orbits. The equations of motion for the coupled orbit/attitude motion were derived and decoupled through the use of a central bus mass. We demonstrated that when assigning reflectivity coefficients or lightness numbers to the two tip masses, artificial unstable equilibria can be generated that are different from the well-known pure gravity gradient dumbbell. By controlling the lightness number of the two masses, the dumbbell attitude can be changed in between the full range of equilibria, relative to the local vertical. For certain combinations of lightness numbers, the stable equilibria even transform into unstable ones, similar to a dumbbell configuration with a very large/small mass ratio $\kappa = m_1/m_2$. Motion between and controllability around the new equilibria are demonstrated through heteroclinic connections in the phase space of the problem. We further reintroduced the coupling of the orbit and attitude dynamics by deriving constraints for the two lightness numbers, showing that without the central bus mass, the dumbbell can also be maintained on a circular non-Keplerian orbit using SRP.

VI. ACKNOWLEDGEMENT

This work was funded by the European Research Council Advanced Investigator Grant - 227571: VISIONSPACE: Orbital Dynamics at Extremes of Spacecraft Length-Scale.

REFERENCES

[1] C. R. McInnes. *Solar Sailing: Technology, Dynamics and Mission Applications*. Springer-Praxis Series in Space Science and Technology, 1999.

[2] O. Brown, P. Eremenko, and B. A. Hamilton. Fractionated space architectures: A vision for responsive space. In *4th Responsive Space Conference*. AIAA, 2006.

[3] C. R. McInnes. Delivering fast and capable missions to the outer solar system. *Advances in Space Research*, 34(1):184–191, 2004.

[4] H. Wen, D. P. Jin, and H. Y. Hu. Advances in dynamics and control of tethered satellite systems. *Acta Mechanica Sinica/Lixue Xuebao*, 24(3):229–241, 2008.

[5] H. M. Elmasri and N. H. McClamroch. Dynamics and control properties for an asymmetric dumbbell spacecraft. In *2005 IEEE International Conference on Control Applications, CCA, August 28, 2005 - August 31, 2005*, Proceedings of the IEEE International Conference on Control Applications, pages 364–369. Institute of Electrical and Electronics Engineers Inc.

[6] K. Meyer, G. Hall, and D. Offin. *Introduction to Hamiltonian Dynamical Systems and the N-Body Problem*. Lecture Notes in Computer Science. Springer, 2008.

[7] D.T. Greenwood. *Classical Dynamics*. Dover Books on Physics. Dover Publications, 1997.